Thoron in indoor air: modeling for a better exposure estimate

Abstract Only recently, the radioactive gas thoron (²²⁰Rn) and its decay products have been regarded as significant health risk in the indoor environment. This is because of new findings of increased thoron concentrations in traditional mud dwellings and considerations leading toward reduced action levels for natural airborne radionuclides. A model which describes the sources and sinks of thoron and its decay products should help to assess the indoor exposure. This work presents an extensive depiction of the influences of indoor conditions on the occurrence of these radionuclides. Measurements were performed in an experiment room and in mud dwellings in China and India. Mud even with an average ²³²Th concentration was identified as a significant thoron source. The spatial distribution of the decay products proved to be homogeneous, which is in contrast to thoron gas. The prominent contribution of the unattached and attached decay product ²¹²Pb to the exposure was elaborated. The theoretically derived impact of air exchange and aerosol concentration, which determines the proportion of unattached decay products, could be confirmed. Transfer coefficients of the model were determined. The thoron model with these transfer coefficients predicts annual doses of almost 2 mSv for dwellers of traditional Chinese and Indian mud buildings, confirming the potential health impact of thoron.

O. Meisenberg, J. Tschiersch

Helmholtz Zentrum München, German Research Center for Environmental Health, Institute of Radiation Protection, Ingolstädter Landstr. 1, Neuherberg, Germany

Key words: Thoron; Rn-220; Decay products; Radio-activity; Mud building; Indoor model.

O. Meisenberg

Helmholtz Zentrum München

German Research Center for Environmental Health

Institute of Radiation Protection

Ingolstädter Landstr. 1 85764 Neuherberg

Germany

Tel.: +49-89-3187-2203

Fax: +49-89-3187-3323

e-mail: oliver.meisenberg@helmholtz-muenchen.de

Received for review 30 October 2009. Accepted for publication 20 October 2010.

Practical Implications

The radioactive noble gas radon with its decay products is well known as a health risk. After increased concentrations of the isotope ²²⁰Rn (thoron) have been found in traditional Chinese mud-walled cave dwellings, the need for a model that describes the occurrence of thoron and its decay products indoors has arisen. This work presents such a model from the emergence of thoron in the building material until the decay to the stable ²⁰⁸Pb and discusses the various influences on the occurrence of these nuclides. The model makes possible to predict the exposure of people staying in a room to thoron and its decay products and – combined with a dose model – to calculate their inhalation doses from easily measurable data.

Introduction

The radioactive noble gas radon is well known being a health risk in the indoor environment causing a significant dose to the lungs and other tissue because of its radioactive decay products. Only recently, a pooled analysis of 13 European studies of residential radon and lung cancer proved the association of exposure to radon (representing its decay chain) and the risk of lung cancer. The established linear dose-response relationship remained significant for radon concentrations even below 200 Bq/m³ without any indication of a threshold (Darby et al., 2005). Consistent results were found in combined analysis of case-control studies in North America (Krewski et al., 2005) and Gansu, China (Wang et al., 2002). These findings, among others, gave reason for the World Health Organization (WHO) to

prepare a handbook advising measures for dose reduction even in the case of relatively moderate exposures (WHO, 2009). In the past, studies focused on the exposure to the decay chain of the isotope ²²²Rn (radon), whereas less attention was paid to the isotope ²²⁰Rn (thoron). Because of its short half-life of 55.6 s, in many houses the predominant part of indoor thoron originates from the building material or the contents. For dwellings made of brick or concrete, its contribution to dose is estimated to be in the order of 10–20% of the dose caused by radon (UNSCEAR, 2000). Therefore, thoron was examined only rarely or as a sideaspect in radon measurements (e.g. Steinhäusler, 1996; Stranden, 1980) and has generally not found attention as a health risk. In the light of reduced radon action levels as proposed by the WHO (WHO, 2009), however, the dose contribution of thoron and its decay products

can be crucial for the total residential indoor exposure to ionizing radiation.

Moreover, elevated thoron concentrations have recently been found in residences made of unfired mineral building material as adobe and mudbricks (Sreenath Reddy et al., 2004), or which are dug directly into the soil as on the Central-Chinese Loess Plateau (Shang et al., 2008; Wiegand et al., 2000). Its contribution to the inhalation dose is up to 50% there (Shang et al., 2005). Thus, the need for a model which describes the occurrence of thoron and its decay products indoors has arisen. For its development, the work of Jacobi (1972) can be used as a base. In the 1970s, he formulated a compartment model for the prediction of the concentrations of radon and its decay products in mines. It was adapted to indoor atmospheres by several contributors (Knutson, 1988; Porstendörfer, 1994). Because of its general approach, it can be applied also to thoron. However, the decay modes and half-lives of the nuclides of the thoron decay chain (Table 1) necessitate various significant changes in the model structure. In addition, model parameters describing the transfer between the different compartments might differ from the respective values in the referred radon models.

This study presents a self-contained indoor thoron compartment model, for which the transfer coefficients were tested for potential differences to the values used in radon models. If necessary, new coefficients were determined experimentally and implemented into the model. The experimental results and respective uncertainties are discussed in detail. With the new model, concentrations of thoron and its decay products can be predicted in given rooms with accessible parameters.

Theoretical background

Characteristics of an indoor thoron model

Using the experience of available indoor models for radon (Jacobi, 1972; Knutson, 1988; Porstendörfer, 1994), a model for thoron must reflect the specific properties of thoron and its decay products. The most

important characteristics of thoron and its decay products in regard to modeling are the following:

- As a major source of indoor thoron in many houses (e.g. mudbrick dwellings) is the building material and thus a part of the building, the exhalation of thoron is an essential part of the model. In certain house types, advective transport into the indoor air must be considered as well (Li et al., 1992) despite the short half-life of 55.6 s.
- Thoron will not spread homogeneously inside a room but will feature a spatial distribution, which is governed by its diffusive and advective transport from the walls, because of its short half-life (Shang et al., 2008). Thus, local concentrations do not represent the average concentration in a room. However, the concentrations of its decay products are determined by the average concentration of thoron for which reason the spatial distribution of the gas is of minor relevance for an exposure model. Therefore, it is not taken into account in this work.
- The long half-lives of the decay products (212Pb: 10.6 h, 212Bi: 1.01 h) reduce the importance of the radioactive decay as a sink of these nuclides in favor of the other sinks, which are air exchange, attachment to aerosol particles, and deposition of unattached and attached decay products. Therefore, both the equilibrium factor, which describes the ratio of the concentrations of the decay products to the average concentration of thoron, and the unattached fraction, which is the ratio of the concentrations of unattached to attached decay products, will be smaller and more dependent on the strength of the sinks than it is the case with the radon decay chain.
- Whereas thoron with its short half-life cannot be transported to adjacent rooms, ²¹²Pb can. Therefore, the transport from the crawl space and other rooms must be regarded as a source of ²¹²Pb.
- Similar to the exposure to radon and its decay products, the alpha-particle emission of the thoron decay products accounts for the overwhelming portion to the inhalation dose. Therefore, the potential alpha-energy concentration *PAEC*, which is the total

Table 1 Half-lives and decay modes of the nuclides of the thoron decay chain as well as their weight in the total potential alpha energy of the decay chain

Nuclide	Half-life (Firestone et al., 1996)	Decay constant [s ⁻¹]	Decay mode	PAE/activity [nJ/Bq]	Weighting factor for total <i>PAE</i> of decay chain
²²⁰ Rn	55.6 s	1.25×10^{-2}	alpha	0.27	
²¹⁶ Po	145 ms	4.78	alpha	4.9×10^{-4}	6.5×10^{-6}
²¹² Pb	10.6 h	1.82×10^{-5}	beta	69.1	0.913
²¹² Bi	1.01 h	1.91×10^{-4}	alpha (36%) to ²⁰⁸ TI beta (64%) to ²¹² Po	6.56	0.087
²¹² Po	299 ns	2.32×10^{3}	alpha	6.1×10^{-10}	8.1×10^{-12}
²⁰⁸ TI	3.05 min	3.79×10^{-3}	beta	0	0
Total				75.6	

energy of the alpha-particles emitted by the decay products per volume, is a suitable measure of the exposure to thoron and its decay products. The long-lived decay products ^{212}Pb and – to a much smaller extent – ^{212}Bi contribute almost completely to the PAEC of the thoron decay chain (Table 1). Therefore, a thoron exposure model must focus on these nuclides, whereas ^{216}Po (in equilibrium with thoron), ^{212}Po (because of its short half-life), and ^{208}Tl (PAEC=0) can be disregarded.

An appropriate structure of such a model is shown in Figure 1, which takes into account the earlier discussed properties. At first, the transfers between the compartments will be described by the solutions of differential equations, which will be derived theoretically; a more detailed treatment of the theoretical background can be found in Meisenberg and Tschiersch (2010). Thereafter, the transfer coefficients occurring in these equations will be provided by measurement results, which will cover a detailed determination of the influences on the thoron exhalation, of the coefficient of attachment of the decay products to aerosol particles, and of their deposition velocity. Additionally, an important input parameter for dose calculations is the size distribution of the attached decay products.

Average concentration of thoron

Because of its short half-life, in most cases the only source of indoor thoron is its exhalation from the building material or from the foundation but not the transport from adjacent rooms. Air exchange with outdoor air is only relevant as a sink at high air

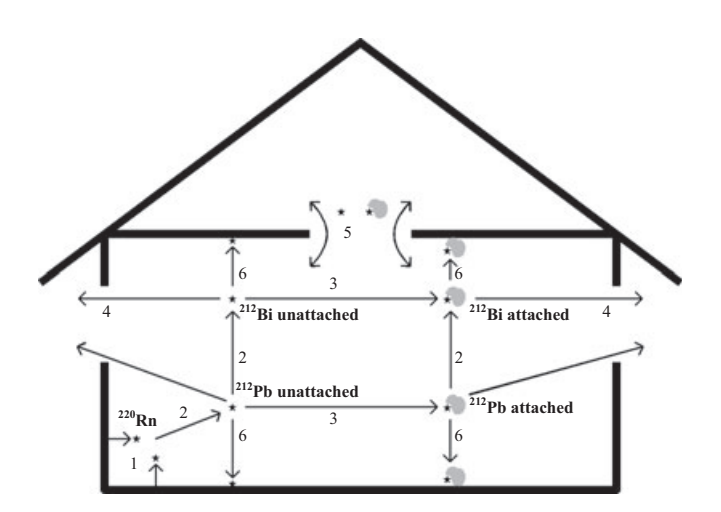


Fig. 1 The five compartments of an indoor thoron model (220 Rn and 212 Pb and 212 Bi in the unattached state and attached to aerosol particles) and possible transfers between them: 1: exhalation from the building material, 2: radioactive decay, 3: attachment to aerosol particles (gray blots), 4: air exchange with outdoor air, 5: air exchange with adjacent rooms, 6: deposition onto surfaces. Radioactive decay to 212 Bi, which is not illustrated in the figure, is an additional sink to this nuclide

exchange rates. Then, its average concentration $\bar{c}_{\rm Tn}$ [Bq/m³] is described by the following differential equation:

$$\frac{d\bar{c}_{Tn}}{dt} = \frac{E \cdot S_{Tn}}{V} - \lambda_{Tn} \cdot \bar{c}_{Tn} - aer \cdot \bar{c}_{Tn}$$
 (1)

with t [s] as time, E [Bq/m²/s] as the exhalation rate, S_{Tn} [m²] as area of thoron exhaling surfaces, V [m³] as the volume of the room, λ_{Tn} [s⁻¹] as the decay constant of thoron, and aer [s⁻¹] as the air exchange rate.

In the state of equilibrium, the solution of this equation yields the average concentration of thoron in the room:

$$\bar{c}_{\mathrm{Tn}} = \frac{E \cdot S_{\mathrm{Tn}}}{(\lambda_{\mathrm{Tn}} + aer) \cdot V},\tag{2}$$

where the air exchange rate aer can be neglected in most cases.

If the spatial distribution $c_{\rm Tn}(\mathbf{r})$ [Bq/m³] of thoron in the room is known from measurements at different positions, the average concentration can also be calculated as the integral of the thoron concentration over the volume V [m³]:

$$\bar{c}_{\rm Tn} = \frac{1}{V} \cdot \int_{V} c_{\rm Tn}(\mathbf{r}) \, \mathrm{d} \, \mathbf{r}. \tag{3}$$

Concentrations of ²¹²Pb and ²¹²Bi

As the long-lived 212 Pb can disperse homogeneously in a room, its concentration does not depend on the local but on the average concentration \bar{c}_{Tn} [Bq/m³] of its preceding nuclides 216 Po and thoron. Additionally, 212 Pb in one room can be caused by air exchange with another room which contains 212 Pb (air exchange rate aer^* [s⁻¹], concentration $c_{^{212}$ Pb aer [Bq/m³]). Sinks of 212 Pb are radioactive decay (decay constant $\lambda_{^{212}$ Pb [s⁻¹]), air exchange with outdoor air (air exchange rate aer [s⁻¹]), deposition onto surfaces (deposition rate δ [s⁻¹]), and possible further sinks such as filtration (rate σ [s⁻¹]). Thus, the differential equation which describes the concentration $c_{^{212}$ Pb [Bq/m³] of indoor 212 Pb is

$$\frac{dc_{212Pb}}{dt} = \lambda_{212Pb} \cdot \bar{c}_{Tn} + aer^* \cdot c_{212Pb\,aer} - (\lambda_{212Pb} + aer + \delta + \sigma) \cdot c_{212Pb}.$$
(4)

In many cases, dwellings with several rooms can be considered as one spatial compartment with one average concentration of ²¹²Pb. Then, air exchange with adjacent rooms as a source of ²¹²Pb does not apply, and the solution of the differential equation in the state of equilibrium is

$$c_{^{212}\text{Pb}} = \frac{\lambda_{^{212}\text{Pb}} \cdot \bar{c}_{\text{Tn}}}{\lambda_{^{212}\text{Pb}} + aer + \delta + \sigma}.$$
 (5)

Similarly, the concentration $c_{^{212}\text{Bi}}$ of ^{212}Bi [Bq/m³] is given by

$$c_{^{212}\text{Bi}} = \frac{\lambda_{^{212}\text{Bi}} \cdot c_{^{212}\text{Pb}}}{\lambda_{^{212}\text{Bi}} + aer + \delta + \sigma}.$$
 (6)

With the comparatively long half-lives of ²¹²Pb and ²¹²Bi, air exchange and deposition play more important roles as sinks for the decay products of thoron than for those of radon.

Unattached fraction of the decay products

Similarly to the calculation of the total concentration of ^{212}Pb , the equilibrium concentrations of the nuclide in the unattached and the attached state ($c_{^{212}\text{Pb}\,\text{unatt}}$ and $c_{^{212}\text{Pb}\,\text{att}}$) can be calculated from the respective differential equations:

$$\frac{\mathrm{d} c_{212} p_{\text{b unatt}}}{\mathrm{d} t} = \lambda_{212} p_{\text{b}} \cdot \bar{c}_{\text{Tn}} - \left(\lambda_{212} p_{\text{b}} + aer + \delta_{\text{unatt}} + \sigma + \bar{\beta} Z\right) c_{212} p_{\text{b unatt}}, (7)$$

$$\frac{\mathrm{d} c_{212} p_{\text{batt}}}{\mathrm{d} t} = \bar{\beta} Z \cdot c_{212} p_{\text{bunatt}}(t) - (\lambda_{212} p_{\text{b}} + aer + \delta_{\text{att}} + \sigma) \cdot c_{212} p_{\text{batt}}$$
(8)

$$\overrightarrow{c}_{212\text{Pb unatt}} = \frac{\lambda_{212\text{Pb}} \cdot \overline{c}_{\text{Tn}}}{\lambda_{212\text{Pb}} + aer + \delta_{\text{unatt}} + \sigma + \overline{\beta}Z},$$
 (9)

$$c_{^{212}\text{Pb att}} = \frac{\bar{\beta}Z \cdot c_{^{212}\text{Pb unatt}}}{\lambda_{^{212}\text{Pb}} + aer + \delta_{\text{att}} + \sigma},$$
(10)

$$f_{P^{212}Pb} \equiv \frac{c_{212}P_{b\,unatt}}{c_{212}P_{b\,unatt} + c_{212}P_{b\,att}}$$

$$= \frac{c_{212}P_{b\,unatt}}{c_{212}P_{b\,unatt} + \frac{\bar{\beta}Z \cdot c_{212}P_{b\,unatt}}{\lambda_{212}P_{b} + aer + \delta_{att} + \sigma}}$$

$$= \frac{\lambda_{212}P_{b} + aer + \delta_{att} + \sigma}{\lambda_{212}P_{b} + aer + \delta_{att} + \sigma + \bar{\beta}Z},$$
(11)

with $\delta_{\rm unatt}$ and $\delta_{\rm att}$ [s⁻¹] as the deposition rates of ²¹²Pb in the unattached and the attached state, respectively, $\bar{\beta}$ [cm³/s] as the average rate of attachment to aerosol particles and Z [cm⁻³] as the aerosol concentration. Its long half-life gives ²¹²Pb more time to attach to

Its long half-life gives ^{212}Pb more time to attach to aerosol particles. Therefore, the unattached fraction $f_{\text{P}^{212}\text{Pb}}$ of ^{212}Pb is expected to be smaller than that of the radon decay products. The rates of the other sinks, especially the air exchange rate, influence the unattached fraction at equal aerosol concentrations significantly.

The unattached fraction $f_{\rm P^{2l2}Bi}$ of $^{2l2}{\rm Bi}$ is even smaller than that of $^{2l2}{\rm Pb}$ as only further attachment, but no separation from aerosol particles occurs. With the much smaller contribution of $^{2l2}{\rm Bi}$ to the potential alpha-energy concentration of the thoron decay chain,

the contribution of unattached 212 Bi can be disregarded. Then, the total unattached fraction f_P of the thoron decay chain is:

$$f_{\rm P} = k_{^{212}\rm Pb} \cdot f_{\rm P}{}^{_{212}\rm Pb} + k_{^{212}\rm Bi} \cdot f_{\rm P}{}^{_{212}\rm Bi} \approx k_{^{212}\rm Pb} \cdot f_{\rm P}{}^{_{212}\rm Pb}$$

$$\tag{12}$$

with k_i as the weighting factor of nuclide i in the decay chain (cf. last column in Table 1).

Materials and methods

Clay buildings

It was found that thoron is an indoor problem in dwellings made of unfired mineral building material as mud (Shang et al., 2008; Sreenath Reddy et al., 2004). Therefore, the test room for the determination of the transfer coefficients for the compartment model should represent such type of dwellings. An experimental room with thoron exhaling walls, ceiling, and floor was erected inside a laboratory at Helmholtz Zentrum München. It is built from commercially available mudbricks (Claytech, Germany) and features dimensions of l = 280 cm, w = 154 cm, and peak height h = 177 cm; its volume is 7.1 m³. The room has a semicylindrical vault (a barrel vault) and two closable windows (0.14 m² each) and one door (0.43 m²) in one of the long sides; thus, it patterns the typical shape of traditional Chinese above-ground cave dwellings (Wang et al., 1996). The inner plaster (Claytech, Germany) was mixed with a powder of thoriumrich Thanstein granite (Wiegand, 1993; grain size < 0.1 mm, mass ratio of the mixture: 3%) and then applied with a thickness of 4.2 cm; its specific ²³²Th activity is about 50 Bq/kg. The surface of the plaster is 21 m², its density 1800 kg/m³, and its porosity is 25%. More details are given by Tschiersch and Meisenberg (2010).

The air exchange rate of the experimental room was controlled by opening or closing its door and its windows more or less. High aerosol concentrations in the room (>15 000/cm³) were obtained by burning a candle in the room without forced air mixing; reported aerosol concentrations are averaged over at least one day. Low aerosol concentrations (<6 000/ cm³) were achieved by filtration of the air inside the experimental room and in the surrounding laboratory until the desired aerosol concentration was reached. Later, only the air in the laboratory was filtered until the end of the measurement to keep the aerosol concentration constant without affecting the decay product concentration inside the experimental room. Measurements inside the experimental room were started not until the decay product concentration there reached its state of equilibrium after the filtration in the experimental room. The laboratory which the experimental room is situated was ventilated well without drafts to prevent any advection of the long-lived decay products back into the experimental room. The temperature in the experimental room was between 20 and 25 °C, which was achieved by heating the laboratory room. The humidity was about 40% without artificial influence.

Measurements of the concentrations, deposition velocities, and size distributions of thoron decay products as well as of indoor atmospheric quantities such as air exchange rate and aerosol concentration were performed inside the experimental room. Results which were gained from these measurements were compared with measurements in Chinese and Indian rooms in which increased thoron concentrations were found. In the Central-Chinese Loess Plateau, many people still live in caves, which are dug into the steep slopes of the prevalent canyons or into the walls of excavated yards (Wang et al., 1996). Usually, they are several meters long and have only a small door and windows at the side facing the canvon or the vard. Larger and more modern houses feature separate single-story rooms built from mudbricks with barrel vaults and a floor of rammed earth; they are called above-ground cave dwellings. Measurements were performed in an above-ground cave dwelling (length: 6.3 m, width: 3.4 m, height: 4.0 m), which is located close to the city of Jingchuan, Gansu province, in continental climate with average temperatures between -5 and 23 °C.

In the northern provinces of India, single- or two-story buildings from mudbricks are prevalent. In contrast to the Chinese above-ground cave dwellings, ceilings and floor are built from different materials such as wood. Rooms are in general several meters long and wide and 2 to 3 m high. Measurements were performed in several such rooms. The rooms in China as well as those in India were unoccupied during the measurements. The indoor conditions were left unaffected to get results which can be transferred to usual exposure situations.

Measurement of thoron exhalation rates

Measurements of thoron exhalation rates from samples were conducted with the common radon and thoron measurement device Rad-7 (Durridge, USA). It uses the electrostatic deposition of thoron decay products. Air is conveyed with a volume flow rate of about 1 l/min from the end of an inlet tube. For the exhalation rate measurements, it was connected in closed circuit to an air-tight chamber containing the sample, a so-called accumulation chamber (Tuccimei et al., 2006). The exhalation rate E [Bq/m²/s] can be calculated as

$$E = \frac{c_{\text{Tn}} \cdot V \cdot \lambda_{\text{Tn}}}{S} \tag{13}$$

with

 c_{Tn} [Bq/m³] as the measured thoron concentration, V [m³] as the volume of the closed circuit,

 $\lambda_{Tn} [s^{-1}]$ as the decay constant of thoron,

S [m²] as the thoron exhaling surface of the sample. Possible small leakage of thoron from the chamber and back-diffusion into the sample can be neglected because of the short half-life of the nuclide.

Except of the measurement of the exhalation rate as a function of the sample thickness, all samples were at least 2 cm thick. Samples of building material were sealed with thoron-proof acrylic lacquer, which contains synthetic resin as binding agent, in two layers on all sides but one to provide exhalation to only one side as it is the case with a wall plastering or a floor: comparative measurements showed a reduction of the exhalation rate by a factor of about 70 after applying the lacquer. Unless otherwise noted, the humidity inside the chamber was set to about 50% as a supersaturated solution of NH₄NO₃ was added to the chamber. Other humidities were achieved with different salts. All samples stayed in the chamber for at least one day before measurements for adaptation of the moisture content to the respective humidity.

Measurement of concentrations of thoron decay products

Working level monitors (commercially available from Tracerlab, Germany; Peter, 1994; Meisenberg and Tschiersch, 2009) were used for the measurement of unattached and total thoron decay product concentrations. The decay products were deposited on a sampling substrate with an airflow rate of about 2.5 l/min. The activity of ²¹²Po (8.8 MeV) on the substrate was measured online by alpha-spectrometry and yields the airborne concentrations of its longer-lived mother nuclides ²¹²Pb und ²¹²Bi (represented by their potential alpha-energy concentration) in total. The measurement efficiency was calibrated with an ²⁴¹Am standard source in place of the substrate; the airflow rate measurement was calibrated using a bubble flow meter, which is traceable to a NIST standard. The working level monitors inevitably disturbed the air around their sampling location, which must be considered for the spatial distribution of the decay products at low air mixing conditions.

For the deposition and measurement of the total thoron decay product concentration, a cellulose nitrate filter (pore size $0.8~\mu m$) was used as the sampling substrate. A wire screen with a mesh size of 625 μm was applied as the sampling substrate for the measurement of unattached decay products (Meisenberg and Tschiersch, 2009). With the given airflow rate, this screen features a negligible deposition probability for attached decay products, whereas unattached decay products are sampled with an efficiency of about 40%, which was calculated according to Cheng et al. (1980).

Measurement of deposition velocities of thoron decay products

The deposition of ²¹²Pb as the dominating thoron decay product was measured as deposition directly onto the surface of planar silicon alpha-spectrometry detectors (diameter: 6.5 cm; Sarad, Germany). Two detectors of the same design were used simultaneously and positioned in the middle of the room in such a way that their surfaces were facing into two of the three different directions of deposition (upwards, downwards or sidewards). Schmidt and Hamel (2001) found no influence of the surface microstructure on the deposition velocity, for which reason the measured deposition velocity can be transferred to the deposition onto the surfaces of the respective room. Deposition onto the detector by special processes as impaction, electrophoresis, and thermophoresis were eliminated by using a large enough detector, grounding the detector, and avoiding temperature variations inside the room, respectively.

The deposition velocity $v_{\rm dep}$ [m/s] of unattached and attached $^{212}{\rm Pb}$ in total, where the contribution of the two states depends on the unattached fraction, can be calculated from the activity of the nuclide on the detector (measured using the alpha decays of $^{212}{\rm Po}$, whose activity on the detector is 64% of that of $^{212}{\rm Pb}$; cf. Table 1) in its equilibrium of deposition and radioactive decay:

$$v_{\text{dep}} = \frac{\varphi}{c_{212\text{Pb}}} = \frac{\lambda_{212\text{Pb}} A}{S_{\text{det}} c_{212\text{Pb}}} = \frac{\lambda_{212\text{Pb}} N}{S_{\text{det}} c_{212\text{Pb}} T \eta b}$$
(14)

with

 φ [Bq/m²/s] as the activity flow rate of decay products onto the detector,

 $c_{^{212}\text{Pb}}$ [Bq/m³] as the concentration of airborne 212 Pb, which was measured by a working level monitor in the middle of the room,

 $\lambda_{^{212}Pb}~[s^{-1}]$ as the decay constant of $^{212}Pb,$

A [Bq] as the activity of 212 Pb on the detector,

 S_{det} [m²] as the surface of the detector,

N as the number of counts from the decay of 212 Po during the measurement,

T [s] as the measurement time,

 $\eta = 0.5$ as the measurement efficiency (2π geometry),

b = 0.64 as the branching in the decay from ²¹²Bi to ²¹²Po.

The deposition rate δ [s⁻¹] is given as

$$\delta = v_{\text{dep}} \cdot S/V \tag{15}$$

with $S[m^2]$ as the surface of the room and $V[m^3]$ as its volume.

²¹²Bi also deposits onto the detector. However, the activity which builds up on the detector by deposition is proportional to the half-life of the nuclide. If airborne ²¹²Bi (half-life of 1.01 h) and ²¹²Pb (half-life of 10.6 h) were in equilibrium and if similar deposition

velocities are assumed, 212 Bi contributes 1.01/10.6 = 9.5% of the total activity. With a typical ratio between the airborne concentrations of both nuclides of 50% this value decreases to only less than 5%. Thus, the influence of the deposition of 212 Bi is small.

Measurement of activity size distributions of attached ²¹²Pb

Attached ²¹²Pb was classified according to its size with a Berner impactor (model LPI 30/0.06, Hauke, Austria) at an airflow rate of 30 l/min. The cut-off diameter of the first stage was 60 nm. The aerosol particles were deposited on aluminum foils, which were dissolved in HCl and analyzed by gamma-spectrometry. The concentration $c_{^{212}\text{Pb}}$ [Bq/m³] of airborne ²¹²Pb of each size class can be calculated from the activity $A_{^{212}\text{Pb}}$ [Bq] in the sample:

$$c_{212Pb} = \frac{A_{212Pb}\lambda_{212Pb}}{k\nu},$$

$$k = 1 - \exp(-\lambda_{212Pb} \cdot T_{\text{sampl}})$$
(16)

with

 $\lambda_{212\text{Pb}}$ [s⁻¹] as the decay constant of ²¹²Pb,

k as a correction factor which describes to which fraction of the equilibrium value the activity on the foil has increased,

 $v \text{ [m}^3/\text{s]}$ as the airflow rate,

 T_{sampl} [s] as the length of the sampling.

Further measurement methods

Measurements of specific activities of ²³²Th in solid samples were conducted by gamma-spectrometry. The results can be traced back to standards provided by PTB (Braunschweig, Germany; German national metrology authority).

Air exchange rates of rooms were measured in the middle of the experimental room temporally separated from other measurements by one-time release of CO₂ as a tracer gas to the indoor air. After a few minutes of reaching a homogeneous distribution of at least 30 000 ppm, the concentration of the homogeneously spread CO₂ decreased by air exchange with clean ambient air featuring a decreasing exponential function. The rate of decrease is the air exchange rate. Reported uncertainties cover 95% of the results from repeated measurements of the air exchange rate at the respective applied condition (i.e. opening of the door and the windows).

Aerosol number concentrations were measured using a condensation particle counter (3022A, TSI, USA) with a lower cut-off diameter of 7 nm and an airflow rate of 18 l/h.

The moisture content of mud samples was measured by weighing the samples after three days of drying at 105 °C and at the respective air humidity.

The content of carbonates in mud was measured using the method of Scheibler (von Soos and Boháč, 2002).

Results and Discussion

Influences on the exhalation of thoron from mud

Specific activity of ^{232}Th . Various samples of mud as a building material (such as mudbricks, rammed earth, plaster) were examined regarding their specific activity $A_{\rm spec}$ [Bq/kg] of 232 Th and their thoron exhalation rate E [Bq/m²/s] (Figure 2). The measurement results can be approximated by a linear function (determination coefficient $R^2 = 0.77$, level of confidence of 95% for all uncertainties):

$$E = (0.031 \pm 0.003) \cdot A_{\text{spec}}.\tag{17}$$

These exhalation rates are in the same order of magnitude as those which are described in existing literature: Sharma and Virk (2001) measured exhalation rates of $11.5 \pm 2.6 \text{ Bq/m}^2/\text{s}$ in mudbricks. Tuccimei et al. (2006) determined exhalation rates of about $1 \text{ Bq/m}^2/\text{s}$ from volcanic rocks and of $6.3 \text{ Bq/m}^2/\text{s}$ from a sample of black pozzolana; these samples featured specific activities of 232 Th of 350 Bq/kg. The European Commission (1999) surveyed natural building stones in the European Union and reports an average specific activity of 232 Th of 60 Bq/kg and a maximum of 310 Bq/kg.

Sample thickness. The influence of the thickness of a dry mud layer made of loam such as plaster on the thoron exhalation rate was observed with two samples, which were several centimeters thick at the beginning; their density was 1750 kg/m³. From measurement to measurement, a few millimeters of clay were carefully removed at the rear side of the sample, which was sealed with thoron-proof lacquer after each time clay had been removed. Figure 3 shows that the thoron

exhalation rate does not decrease until thicknesses of < 2 cm.

If diffusion is restricted to one side of the building material as it is the case for the short-lived thoron, the exhalation rate E [Bq/m²/s] of thoron is given as a function of its thickness d [m] by the following formula (after Jonassen and McLaughlin, 1980; cited in Stranden, 1988):

$$E(d) = \lambda_{\rm Tn} A_{\rm spec} \rho \eta L \tanh\left(\frac{d}{L}\right) \tag{18}$$

with

 $\lambda_{\rm Tn}~[{\rm s}^{-1}]$ as the decay constant of thoron, $A_{\rm spec}~[{\rm Bg/kg}]$ as the specific activity of $^{232}{\rm Th}$,

 ρ [kg/m³] as the density of the sample,

 η as the emanation coefficient,

L [m] as the diffusion length.

This equation was fitted to the measured exhalation rates with the diffusion length L as the fitting parameter $(R^2 = 0.43, \text{ Figure 3})$; the value E(0) = 0 originates directly from Equation 18. The fitting yields a diffusion

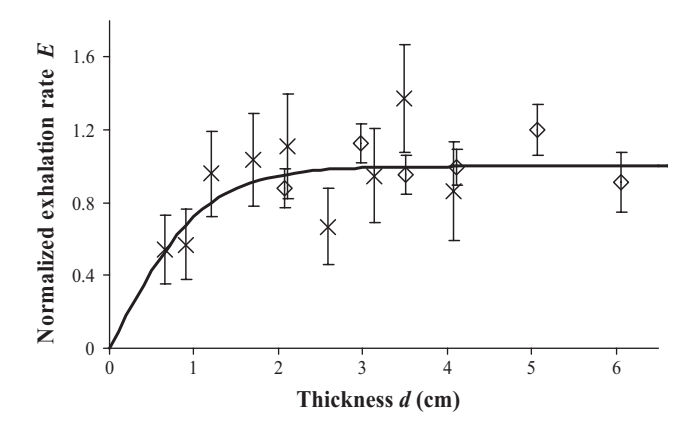


Fig. 3 Exhalation of thoron from two adobe samples as a function of the sample thickness (measured values and fitted curve with the diffusion length L as the fitting parameter)

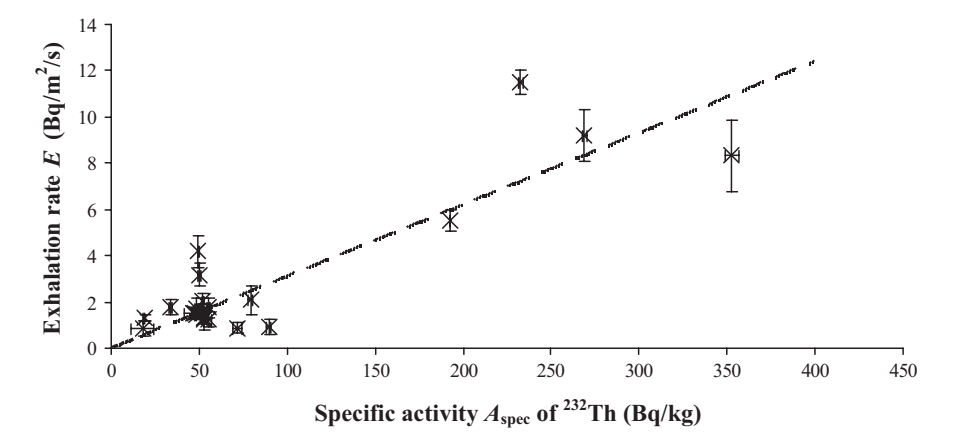


Fig. 2 Thoron exhalation from clay as building material as a function of the specific activity of 232 Th (measured values and linear regression line ($R^2 = 0.77$) according to Equation 17)

length of thoron in the clay of $L=1.1\pm0.3$ cm. This results in an effective diffusion coefficient in the material

$$D_{\rm e} = \frac{L^2}{2\tau} = 0.008 \pm 0.004 \,\,\text{cm}^2 \,\,\text{s}^{-1} \tag{19}$$

with $\tau = 80.2$ s as the mean lifetime of thoron.

Nazaroff et al. (1988) summarize the results of various measurements of the effective diffusion coefficient of radon in dry loam as 0.008 cm²/s. This is in good agreement with the result for mud and thoron, thermodynamic properties of which are similar to those of radon. Yet, the respective diffusion length of radon is 90 cm and thus larger than the thickness of common walls.

The measured diffusion length makes possible to calculate the emanation coefficients of the various mud samples presented in Figure 2, which are sufficiently thicker than the diffusion length $(\tanh(d/L) \approx 1)$. The emanation coefficients are in the range from 20 to 80% and are thus greater than thoron emanation coefficients of other materials found in literature: Megumi and Mamuro (1974) measured emanation coefficients between 0.09 and 0.15 in dried soil. Porstendörfer (1994) summarizes results of several measurements of building material (concrete, fired bricks) between 0.2 and 6%. The strong exhalation of thoron from mud can be explained by the exceptionally thin and flat structure of clay mineral grains, which consist of phyllosilicates, as its main constituent (Grim, 1968). Thoron atoms, which emerge in the grains, can easily reach a pore by their recoil as a consequence of the alpha-decay of the mother nuclide, whereas in minerals with greater grain size they are more likely to be stopped in the same grain.

Humidity. The dependence of the thoron exhalation on the humidity of the ambient air was observed by exhalation rate measurements in different humidity with two samples. Reduced exhalation rates down to about 20% of the saturation value were measured at low humidity of about 2%. The saturation value was reached at humidity greater than 5% with one sample, but only at humidity > 30 to 40% with the other sample. High humidity close to 100% (moisture content of the samples of about 5%) did not lead to reduced exhalation rates, which is different from the results found for thoron from granitic soil by Hosoda et al. (2007).

Firing of mudbricks. To measure the influence of firing on the exhalation of thoron from mud as a building material, three samples of mudbricks of low carbonate content (1–5%) were fired for three days at 900 °C. After cooling and accommodating in the humid air of the accumulation chamber, the exhalation rate was measured. Its relative value compared to that before the firing was $6.4 \pm 5.1\%$ on average. Thus, these fired

bricks exhale thoron much less than sun-dried mudbricks with equal specific activity of ²³²Th and constitution. This is because during the firing part of the minerals in the mud melt and obstruct the pores, preventing thoron to diffuse out of the brick (Cultrone et al., 2004).

Behavior of the decay products

Spatial distribution. The spatial distribution of the thoron decay products concentration was determined by simultaneous measurements at a position of particularly great thoron concentration, i.e. in a corner of the room at a distance of 2 cm to the walls and the floor, and in the middle of the room. Each time a measurement result was gained, the ratio of these values was calculated. At the very small air exchange rate of 0.1/h with the only disturbance of the air caused by the active sampling, the average ratio of the concentrations was observed as 1.07 ± 0.04 . At an air exchange rate of $12 \pm 3/h$, a twelve-day measurement did not yield a significant difference in the concentrations; the average ratio was 1.00 ± 0.08 . Thus, thoron decay products can be considered to be distributed homogeneously in indoor air. A measurement of their concentration at one place in the room is representative for the whole room. However, the spatial distribution of unattached ²¹²Pb needs separate investigation.

Deposition velocity. The velocity of the upward, downward, and sideward deposition of unattached and attached ²¹²Pb in total in the experimental room as a function of the unattached fraction, which was measured simultaneously, is shown in Figure 4. Independent on the direction of the deposition, a linear relation could be found. It can be written as the sum of the deposition velocity of unattached ²¹²Pb on the one hand and attached ²¹²Pb on the other hand:

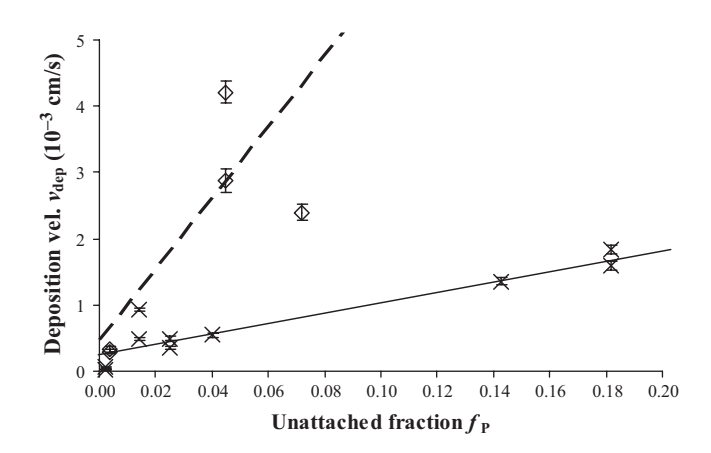


Fig. 4 Deposition velocity of the thoron (X) and radon (\diamondsuit) decay products as a function of the unattached fraction (together with lines of linear regression according to Equation 20 with $v_{\rm dep\ unatt}$ and $v_{\rm dep\ att}$ as the fitting parameters)

$$v_{\rm dep} = v_{\rm dep \, unatt} \cdot f_{\rm P} + v_{\rm dep \, att} \cdot (1 - f_{\rm P}) \tag{20}$$

with

 v_{dep} , $v_{\text{dep unatt,}}$ and $v_{\text{dep att}}$ [m/s] as the deposition velocities of the total, unattached, and attached ²¹²Pb, respectively,

 $f_{\rm P}$ as the unattached fraction.

By extrapolation to $f_{\rm P}=1$ and $f_{\rm P}=0$, $v_{\rm dep\ unatt}=(7.7\pm0.5)\times10^{-3}$ cm/s and $v_{\rm dep\ att}=(3.1\pm0.6)\times10^{-4}$ cm/s can be determined.

Mishra et al. (2009) applied a deposition model and calculated a similar deposition velocity of 2.6×10^{-4} cm/s for attached ²¹²Pb in horizontal direction, whereas their respective value of 7.1×10^{-2} cm/s for the unattached state could not be confirmed.

Literature presents deposition velocities of radon decay products, which differ by about one order of magnitude from each other. Schmidt and Hamel (2001) found average deposition velocities of unattached radon decay products of 4.8×10^{-2} cm/s for 214 Pb and 1.2×10^{-2} cm/s for 214 Bi. Knutson (1988) summarizes the results of several measurements between 1.4 and 2.8×10^{-1} cm/s for the unattached state and between 8×10^{-4} and 6×10^{-3} cm/s for the attached state. The deposition velocities of radon decay products from this work (unattached: $(5.4 \pm 1.2) \times 10^{-2}$ cm/s, attached: $(4.7 \pm 2.4) \times 10^{-4}$ cm/s), which were measured simultaneously, confirm the order of magnitude of the values from literature. The deposition velocities of ²¹²Pb from the thoron decay chain, however, are smaller than these values: a certain unattached fraction of thoron decay products occurs at a smaller aerosol concentration than the same unattached fraction of radon decay products. Thus, the mean lifetime of unattached thoron decay products until attachment is longer than that of unattached radon decay products. Chen et al. (1997) observed a growth of clusters of unattached 212Pb during their aging; older clusters of unattached decay products are larger and thus feature a smaller diffusion velocity than younger clusters.

Unattached fraction. The unattached fraction of the thoron decay products in total was measured at various aerosol concentrations in the experimental room. The air exchange rate was 0.1/h. Figure 5 displays unattached fractions smaller than 5% for usual aerosol concentrations of at least a few thousand particles per cm³; this is much smaller than usual unattached fractions of radon decay products and can be explained by the longer half-life of the thoron decay products, which gives them more time to attach to aerosol particles. However, greater air exchange rates should result in greater unattached fractions at equal aerosol concentrations because of the shorter lifetime of the decay products in the room (cf. Equation 11).

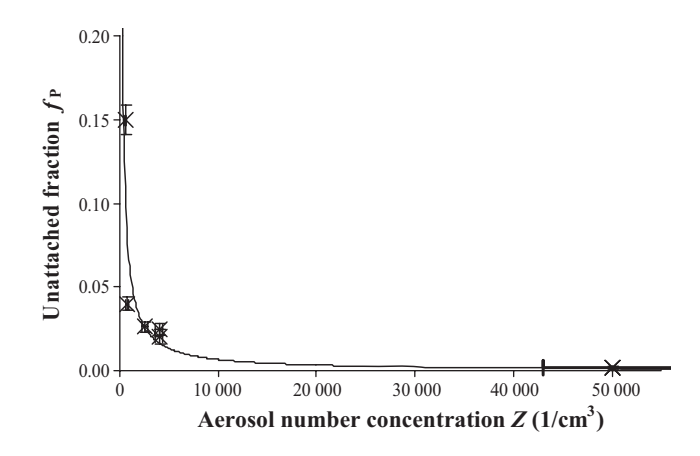


Fig. 5 Unattached fraction of the thoron decay products as a function of the aerosol number concentration (measured values and fitted curve according to Equations 11 and 12 with the attachment coefficient $\bar{\beta}$ as the fitting parameter, $R^2 = 0.75$)

With the measured unattached fractions, the attachment coefficient $\bar{\beta}$ of ²¹²Pb from Equation 11 averaged over the aerosol size distribution can be calculated as $(7.9 \pm 2.1) \times 10^{-7}$ cm³/s (Figure 5), which agrees well with values from literature between 5.6×10^{-7} and 1.4×10^{-6} cm³/s (Mohnen, 1969; Porstendörfer and Mercer, 1978; Porstendörfer and Reineking, 2000).

Size distribution. The activity size distribution of attached ²¹²Pb was measured in the experimental room at several aerosol concentrations. Each set of measured data can be fitted by a mono- or bimodal log-normal distribution:

$$\frac{\mathrm{d} c_{^{212}\mathrm{Pb}}}{\mathrm{d} \log d} \sim \exp\left(-\frac{1}{2 \cdot (\ln \sigma)^2} \left(\ln \frac{d}{\mu}\right)^2\right). \tag{21}$$

Medians μ [nm] and geometric standard deviations σ are presented in Table 2. Porstendörfer (1994) summarizes the activity size distributions of indoor and outdoor thoron decay products from various measurements and states medians between 140 and 390 nm, which agree with the values from this work. The geometric standard deviations shown in Table 2 lie at

Table 2 Medians μ and geometric standard deviations σ of the log-normal size distributions of the attached thoron decay products at different aerosol number concentrations

Aerosol number concentration [cm ⁻³]	μ [nm]	σ
600	381	2.0
2000	554	2.1
6000	259	2.0
6000	279	1.8
0000	2000	1.3
20000 (Source: candle)	236	2.0
Average (without μ = 2000 nm)	340 ± 120	2.0

the lower end of the range of 2.0–3.5 compiled by Porstendörfer, which might be caused by a narrower aerosol size distribution in indoor air. In real rooms, where the size distributions of the aerosol particles and the thoron decay products are unknown, a median diameter of 340 ± 120 nm, which is the average of the measured medians, and a geometric standard deviation of 2 can be assumed.

The airflow rate through the impactor corresponds to a filtration rate of about 0.25/h in the experimental room. Therefore, it strongly influences the concentrations of the long-lived thoron decay products as a sink. However, no significant influence on the aerosol concentration in the room could be observed. Thus, the influence on the attachment to aerosol particles, which is faster than the filtration rate, should have been small. As the outlet air of the impactor was led back into the room, there was no pressure difference between the experimental room and the surrounding laboratory space.

Measurement results from traditional Chinese and Indian dwellings

Equilibrium factor of thoron and its decay products. The equilibrium factor of thoron can be defined as the ratio of the concentrations of the decay products to the average concentration of thoron. The average thoron concentration was calculated from several consecutive measurements of thoron at different positions, in particular at different distances from the thoron exhaling walls, taking into account the size of the volume in which they exist. Equations 5 and 6 describe the equilibrium factor by the influence of the relevant sinks radioactive decay, deposition, and - most important - air exchange. Measurements in the Chinese above-ground cave dwelling and in an Indian mudbrick house could confirm the strong influence of the air exchange predicted by the model according to Equation 5 (Figure 6). The values are in the range of those found by other authors in occupied houses (average values between below 0.01 and 0.09; Ramola et al., 2003; Shang et al., 2005) and are relevantly smaller than those of radon (0.2-0.8; Porstendörfer, 1994).

Unattached fraction of the decay products. The unattached fraction of the thoron decay products was measured in the Chinese above-ground cave dwelling at an air exchange rate of $0.9 \pm 0.2/h$ and at various aerosol concentrations (Figure 7). Small aerosol concentrations could be achieved without filtration of the air; burning cigarettes and incense sticks yielded great aerosol concentrations, which varied much during the measurement because of the great size of the room and the air exchange. The results can well be described by the model (Equation 11) and the attachment coefficient determined in the experimental room.

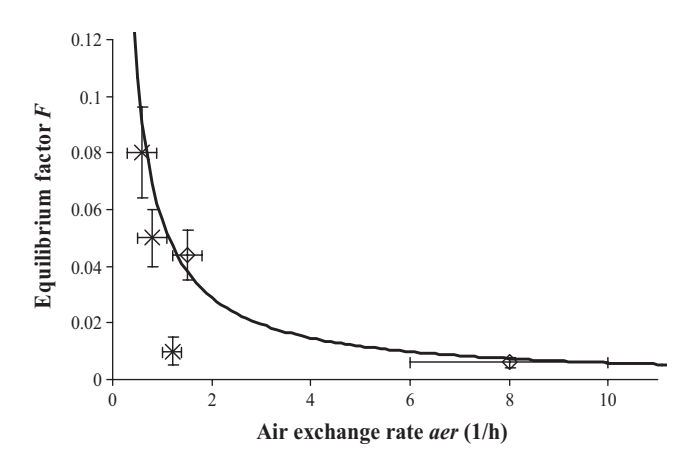


Fig. 6 Influence of the air exchange rate on the equilibrium factor in Chinese (X) and Indian (♦) clay house rooms (experimental results). Solid line: theoretical relation according to Equation 5

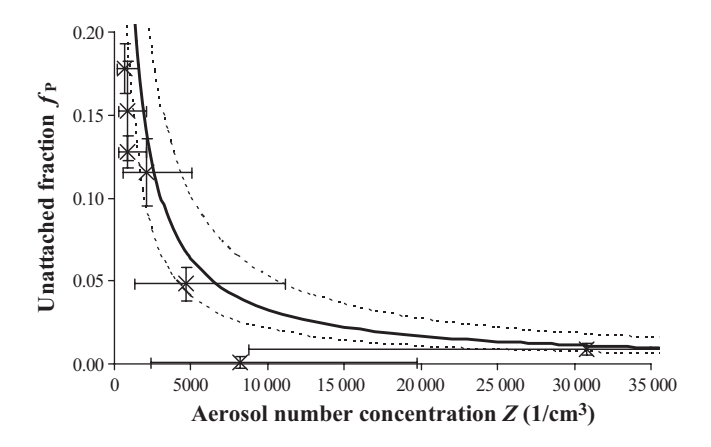


Fig. 7 Unattached fraction of thoron decay products at different aerosol number concentrations in the Chinese above-ground cave dwelling (measured values and prediction by the model, dashed lines: confidence interval of the prediction with level of confidence of 95%)

Application of the model for dose calculations

The determined transfer coefficients can be used for the calculation of the concentrations of thoron and its decay products in their different states with the input parameters to be set by the user of the model. Li et al. (2008) recently published dose coefficients of thoron and its decay products. Applying these values to the concentrations predicted by the model leads to estimates of the inhalation dose of the dwellers caused by thoron and its decay products. Table 3 presents the application of the indoor thoron model with its transfer parameters gained in the experimental room and of the dose coefficients to a Chinese above-ground cave dwelling and an Indian mud house. As the input parameters of the model, constructional and indoor aerial parameters which are typical for such buildings are assumed and therefore do not bear a measurement

Table 3 Application of the model, which uses the measured transfer coefficients to two typical adobe buildings with increased thoron concentrations and assumed usual indoor conditions (applied as exact values without uncertainty): an above-ground cave dwelling in Gansu, China and a room in a dwelling with wooden floor and ceiling in Himachal Pradesh, India

		China	India
Input parameters			
Specific activity of ²³² Th	a [Bq/kg]	50	60
Density of the clay	ρ [kg/m 3]	1500	1800
Volume of the room	$V [m^3]$	78	60
Surface	$S[m^2]$	105	110
Thoron exhaling surface	S_{Tn} [m ²]	105	60
Air exchange rate	aer [h ⁻¹]	0.9	0.6
Aerosol number concentration	Z [cm $^{-3}$]	6000	10000
Output values			
Exhalation rate at great aer	E_0 [Bq/m ² /h]	1.88 ± 0.75	2.70 ± 1.08
Exhalation rate at given aer	E [Bq/m ² /h]	0.64 ± 0.26	0.86 ± 0.34
Thoron activity	A _{Tn} [Bq]	5267 ± 2107	4073 ± 1629
Average thoron concentration	$\bar{c}_{Tn} \; [Bq/m^3]$	68 ± 27	68 ± 27
Conc. of unattached ²¹² Pb	²¹² Pb unatt [Bq/m ³]		0.15 ± 0.06
Conc. of attached ²¹² Pb	²¹² Pb att [Bq/m ³]	4.2 ± 2.0	6.2 ± 3.0
Conc. of attached ²¹² Bi	c ₂₁₂ Bi att [Bq/m ³]	1.8 ± 0.9	3.3 ± 1.6
Unattached fraction	f_{P}	5.0% ± 1.3%	$2.15\% \pm 0.56\%$
Equilibrium factor	F	0.06	0.09
Deposition velocity	$v_{\rm dep} \ [10^{-4} \ {\rm cm/s}]$	6.77 ± 1.08	4.69 ± 0.72
Annual dose			
From thoron and ²¹⁶ Po (middle)	[mSv]	0.02 ± 0.01	0.02 ± 0.01
From unattached ²¹² Pb	[mSv]	0.45 ± 0.18	0.28 ± 0.11
From attached ²¹² Pb	[mSv]	1.03 ± 0.49	1.53 ± 0.73
From attached ²¹² Bi	[mSv]	0.11 ± 0.05	0.20 ± 0.09
Total	[mSv]	1.61 ± 0.53	2.02 ± 0.75

uncertainty. The uncertainties in the output values originate from the uncertainties in the transfer coefficients determined from the measurement results. The input of measured values would yield additional contributions to the uncertainties. In both houses, an annual inhalation dose caused by thoron of up to 2 mSv can be expected if a daily indoor stay of 10 h is assumed. The strongest influence on the concentration of the decay products and thus also on the dose is the air exchange rate. Taking into account the additional exposure to radon of about the same magnitude (Shang et al., 2008), the total exposure to the decay chains of the radon isotopes ²²⁰Rn and ²²²Rn together in the indoor air of mud houses can cause considerable health risks to the dwellers.

Conclusions

The measured values and dependencies describe the strength of all sources and sinks of the three relevant nuclides ²²⁰Rn and unattached and attached ²¹²Pb and ²¹²Bi in indoor atmospheres (Table 4). The derived transfer coefficients, together with the decay constants of the nuclides, complete the theoretically derived structure of the indoor thoron model. Thus, a model is now available to predict concentrations of thoron and its decay products in given rooms which are built of

Table 4 Association of the transfer coefficients to the processes, which are shown in Figure 1. The exhalation rate is given for thoron exhaling clay of a thickness of at least 2 cm and a humidity of at least 30%

Process	Transfer no. (cf. Figure 1)	Quantity	Value
Exhalation	1	Exhalation rate [Bq/m²/s]	$(0.031 \pm 0.003) \cdot A_{\rm spec}$
Radioactive decay	2	Decay constants [s ⁻¹]	220 Rn: 1.25×10^{-2} 212 Pb: 1.82×10^{-5} 212 Bi: 1.91×10^{-4}
Attachment	3	Attachment coefficient [cm ³ /s]	$(7.9 \pm 2.1) \times 10^{-7}$
Air exchange with outdoor air	4	Air exchange rate [h ⁻¹]	Input parameter (typically 0.3–10)
Air exchange with adjacent rooms	5	Air exchange rate [h ⁻¹]	Input parameter (typically 0.3–10)
Deposition	6	Deposition velocity [cm/s]	Unattached: $(7.7 \pm 0.5) \times 10^{-4}$ Attached: $(3.1 \pm 0.6) \times 10^{-4}$

mud. If the thoron exhalation rate is known, it can also be applied to rooms in which different building materials or the soil are the source of indoor thoron. Required input parameters are the room volume, the thoron exhaling and total surface of the room, the specific ²³²Th activity and the thickness of the mud, the air exchange rate, and the aerosol number concentration in the room. The results from original dwellings in China and India used in the validation process are consistent with the model results.

Both model considerations and measurements suggest that measurements of airborne concentrations of the decay products are much more relevant for exposure assessments than measurements of thoron. Several features of the nuclides yield this consequence: The inhomogeneous spatial distribution of thoron prevents its concentrations at a single position in the room to be significant for the average indoor concentration; in contrast ²¹²Pb is homogeneously distributed. Additionally, the strong dependence of the equilibrium factor on the air exchange rate as well as its small values lead to a high uncertainty of exposure assessments even if the average thoron concentration can be calculated. Therefore, measurements for exposure assessments should focus on the decay products or even only on the dominant nuclide ²¹²Pb in the unattached and the attached state.

Acknowledgements

We highly acknowledge the support of Ms. B. Shang of NIRP, Beijing and of Mr. B.S. Bajwa of GND University, Amritsar and their teams at the measurement campaigns in China and India. The campaign in India was partly financed by DAAD (German Academic Exchange Service, Contract No. D/07/03049). We are grateful for the detailed comments by the reviewers of the manuscript.

References

- Chen, T.R., Cheng, Y.S., Hopke, P.K., Tung, C.J. and Pourprix, M. (1997) Electrical mobility and size distribution of aged ²¹²Pb nanometer carriers in nitrogen gas, *J. Aerosol Sci.*, **28**, 1465–1477.
- Cheng, Y.S., Keating, J.A. and Kanapilly, G.M. (1980) Theory and calibration of a screen type diffusion battery, *J. Aerosol Sci.*, **11**, 549–556.
- Cultrone, G., Sebastián, E., Elert, K., José de la Torre, M., Cazalla, O. and Rodriguez-Navarro, C. (2004) Influence of mineralogy and firing temperature on the porosity of bricks, *J. Eur. Ceram. Soc.*, 24, 547–564.
- Darby, S., Hill, D., Auvinen, A., BarrosDios, J.M., Baysson, H., Bochicchio, F.,
 Deo, H., Falk, R., Forastiere, F., Hakama, M., Heid, I., Kreienbrock, L.,
 Kreuzer, M., Lagarde, F., Mäkeläinen, I.,
 Muirhead, C., Oberaigner, W., Pershagen, G., Ruano-Ravina, A., Ruosteenoja,
 E., Rosario, A.S., Tirmarche, M., Tomásek, L., Whitley, E., Wichmann, H.E.
 and Doll, R. (2005) Radon in homes and
 risk of lung cancer: collaborative analysis
 of individual data from 13 European casecontrol studies, *Brit. Med. J.*, 330, 223–
 226.
- European Commission (1999) Radiation protection 112 Radiological protection principles concerning the natural radioactivity of building materials, Luxembourg, Office for Official Publications of the European Communities.
- Firestone, R.B., Shirley, V.S., Chu, S.F., Baglin, C.M. and Zipkin, J. (1996) *Table* of Isotopes – CD ROM Edition, New York, Wiley Interscience.
- Grim, R.E. (1968) *Clay Mineralogy*, New York, McGraw-Hill Book Company.
- Hosoda, M., Shimo, M., Sugimo, M., Furukawa, M. and Fukushi, M. (2007) Effect of soil moisture content on radon and thoron exhalation, J. Nucl. Sci. Technol., 44, 664–672.
- Jacobi, W. (1972) Activity and potential α-energy of ²²²radon- and ²²⁰radondaughters in different air atmospheres, *Health Phys.*, 22, 441–450.
- Jonassen, N. and McLaughlin, J.P. (1980) Exhalation of radon-222 from building materials and walls. In: Gesell, T.F. and Prichard, H.M. (eds) *Natural Radiation Environment III*, Oak Ridge, US Department of Energy, 1211.
- Knutson, E.O. (1988) Modeling indoor concentrations of radon's decay products. In: Nazaroff, W.W. and Nero, A.V. (ed) Radon and its decay products in indoor air, New York, Wiley-Interscience, 161–202.
- Krewski, D., Lubin, J.H., Zielinski, J.M., Alavanja, M., Catalan, V.S., Field, R.W., Klotz, J.B., Létourneau, E.G., Lynch, C.F., Lyon, J.I., Sandler, D.P., Schoenberg, J.B., Steck, D.J., Stolwijk, J.A.,

- Weinberg, C. and Wilcox, H.B. (2005) Residential radon and risk of lung cancer: a combined analysis of 7 North American case control studies, *Epidemiology*, **16**, 137–145.
- Li, Y., Schery, S.D. and Turk, B. (1992) Soil as a source of indoor ²²⁰Rn, *Health Phys.*, **62**, 453–457.
- Li, W.B., Tschiersch, J., Oeh, U. and Hoeschen, C. (2008) Lung dosimetry of inhaled thoron decay products. *Proceedings of IRPA 12*, Buenos Aires, International Radiation Protection Association.
- Megumi, K. and Mamuro, T. (1974) Emanation and exhalation of radon and thoron gases from soil particles, *J. Geophys. Res.*, **79**, 3357–3360.
- Meisenberg, O. and Tschiersch, J. (2009) Online measurement of unattached and total radon and thoron decay products, *Appl. Radiat. Isot.*, **67**, 843–848.
- Meisenberg, O. and Tschiersch, J. (2010) Specific properties of a model of thoron and its decay products in indoor atmospheres, *Nukleonika*, **55**, 463–469.
- Mishra, R., Mayya, Y.S. and Kushwaha, H.S. (2009) Measurement of ²²⁰Rn/²²²Rn progeny deposition velocities on surfaces and their comparison with theoretical models, *J. Aerosol Sci.*, **40**, 1–15.
- Mohnen, V.A. (1969) Die radioaktive Markierung von Aerosolen, *Zeitschrift für Physik A*, **229**, 109–122. (in German).
- Nazaroff, W.W., Moed, B.A. and Sextro, R.G. (1988) Soil as a source of indoor radon: generation, migration, and entry. In: Nazaroff, W.W. and Nazaroff, W.W. (eds), *Radon and its decay products in indoor air*, New York, Wiley-Interscience, 57–112.
- Peter, J.E. (1994) Analysis of radon and thoron daughter concentrations in air by continuous alpha spectroscopy, *Radiat*. *Prot. Dosim.*, **56**, 267–270.
- Porstendörfer, J. (1994) Properties and behaviour of radon and thoron and their decay products in the air, *J. Aerosol Sci.*, **25**, 219–263.
- Porstendörfer, J. and Mercer, T.T. (1978) Concentration distributions of free and attached Rn and Tn decay products in laminar aerosol flow in a cylindrical tube, J. Aerosol Sci., 9, 283–290.
- Porstendörfer, J. and Reineking, A. (2000) Radon characteristics related to dose for different living places of the human. In: *Proceedings of IRPA 10*, Hiroshima, International Radiation Protection Association.
- Ramola, R.C., Negi, M.S. and Choubey, V.M. (2003) Measurement of equilibrium factor "F" between radon and its progeny and thoron and its progeny in the indoor atmosphere using nuclear track detectors, *Indoor Built Environ.*, 12, 351–355.

- Schmidt, V. and Hamel, P. (2001) Measurements of deposition velocity of radon decay products for examination of the correlation between air activity concentration of radon and the accumulated Po-210 surface activity, *Sci. Total Environ.*, **272**, 189–194.
- Shang, B., Chen, B., Gao, Y., Cui, H. and Li, Z. (2005) Thoron levels in traditional Chinese residential dwellings, *Radiat*. *Environ. Biophys.*, 44, 193–199.
- Shang, B., Tschiersch, J., Cui, H. and Xia, Y. (2008) Radon survey in dwellings of Gansu, China: the influence of thoron and an attempt for correction, *Radiat*. *Environ. Bioph.*, **47**, 367–373.
- Sharma, N. and Virk, H.S. (2001) Exhalation rate study of radon and thoron in some building materials, *Radiat. Meas.*, **34**, 467–469.
- von Soos, J. and Boháč, P. (2002)
 Properties of soils and rocks and their laboratory determination. In: Smoltczyk, U. (ed.) *Geotechnical Engineering Handbook Vol. 1*, Berlin, Ernst & Sohn, 119–204.
- Sreenath Reddy, M., Yadagiri Reddy, P., Rama Reddy, K., Eappen, K.P., Ramachandran, T.V. and Mayya, Y.S. (2004) Thoron levels in the dwellings of Hyderabad city, Andhra Pradesh, India, J. Environ. Radioactiv., 73, 21–28.
- Steinhäusler, F. (1996) Environmental ²²⁰Rn: a review, *Environ. Int.*, **22**, S1111–S1123.
- Stranden, E. (1980) Thoron and radon daughters in different atmospheres, *Health Phys.*, **38**, 777–785.
- Stranden, E. (1988) Building materials as a source of indoor radon. In: Nazaroff, W.W. and Nero, A.V. (eds), *Radon and its* decay products in indoor air, New York, Wiley-Interscience, 113–130.
- Tschiersch, J. and Meisenberg, O. (2010) The HMGU thoron experimental house: a new tool for exposure assessment, *Radiat*. *Prot. Dosim.*, **141**, 395–399.
- Tuccimei, P., Moroni, M. and Norcia, D. (2006) Simultaneous determination of ²²²Rn and ²²⁰Rn exhalation rates from building materials used in Central Italy with accumulation chambers and a continuous solid state alpha detector: influence of particle size, humidity and precursors concentration, *Appl. Radiat. Isotopes.*, **64**, 254–263.
- United Nations Scientific Committee on the Effects of Atomic Radiation (2000) Sources and Effects of Ionizing Radiation, Annex B: Exposures from natural radiation sources, New York, United Nations.
- Wang, Z.Y., Lubin, J.H., Wang, L.D.,
 Conrath, S., Zhang, S.Z., Kleinerman, R.,
 Shang, B., Gao, S.X., Gao, P.Y., Lei,
 S.W. and Boice, J.D. Jr (1996) Radon
 measurements in underground dwellings

- from two prefectures in China, *Health Phys.*, **70**, 192–198.
- Wang, Z.Y., Lubin, J.H., Wang, L.D., Zhang, S.Z., Boice, J.D. Jr, Cui, H.X., Zhang, S.R., Conrath, S., Xia, Y., Shang, B., Brenner, A., Lei, S.W., Metayer, C., Cao, J.S., Chen, K.W., Lei, S.J. and Kleinerman, R.A. (2002) Residential
- radon and lung cancer risk in a high-exposure area of Gansu province, China, *Am. J. Epidemiol.*, **155**, 554–564.
- Wiegand, J. (1993) Geochemische und radiometrische Untersuchungen an den Graniten des Neunburg-Thansteiner Massivs (Oberpfalz), Bonn, Bonner Geowissenschaftliche Schriften (in German).
- Wiegand, J., Feige, S., Quingling, X., Schreiber, U., Wieditz, K., Wittmann, C. and Xiarong, L. (2000) Radon and thoron in cave dwellings (Yan'an, China), *Health Phys.*, 78, 438–444.
- World Health Organization (2009) WHO Handbook on Indoor Radon: A Public Health Perspective, Geneva, WHO.